*Research Article*

# Spatial and Temporal Assessment of Meteorological Drought Using the Standardized Precipitation Index (SPI) and Its Effect on Crop Yield Over the Corn Belt Region of the United States from 2000 to 2023

**Victor Araya[1], Mbongowo Mbuh[1,*], Gregory Vandeberg[1] and Jeffrey VanLooy[2]**

[1] Department of Geography and Geographic Information Science, University of North Dakota, Grand Forks, USA;
[2] Earth System Science and Policy, University of North Dakota, Grand Forks, USA
* Corresponding author: mbongowo.mbuh@und.edu ; +1-701-777-4587

**Abstract:** Climate change and global warming have contributed to extreme weather events and patterns, including severe flooding, earthquakes, wildfires, and drought. Drought happens to be the deadliest catastrophic event around the world. Drought's impact on ecosystems and local communities has been increasing in many parts of the world, including the United States and, most importantly, the Corn Belt, which also happens to be the country's food basket. Drought prediction and mitigation can be investigated through drought indices. The standardized precipitation index (SPI) is considered the most reliable in this study. The index is the most reliable as it serves as one of the most fundamental. It is used in this study to present the critical identifier for diagnosing the intensity, duration, and frequency of drought severity. Additionally, SPI is a key identifier in extreme precipitation events. It is comparable to various landscapes across a region and is simple to use concerning its calculation process. This study focuses on the Midwest Corn Belt Region of the United States, between the climate record from 2000–2023. This study is designed to understand precipitation regimes and their impact on cropland cover and yield (condition monitoring and crop progress) over the climate record. Results of the study showed drought affecting portions of the region, especially during the first half of the period, with 2012 indicating peak severity plaguing both corn belts. Generally, pre-2012 and post-2012 indicated the wettest conditions, especially in 2010, 2014, and 2016. While cropland cover highlighted the widespread distribution of corn and soybean cover in both Corn Belts, crop condition and progress corresponded and responded well to low yields during the intense drought years and high yields during the wettest years. Our analysis shows that climate change has undoubtedly resulted in a temperature rise, exacerbating the frequency and severity of heat waves and extreme precipitation events impacting parts of the United States, including the Corn Belt.

**Keywords:** meteorological drought, Corn Belt region, drought indices, standardized precipitation index (SPI), climate change

Academic Editor: Jeong Chang Seong
Received: 15 August 2025
Revised: 22 September 2025
Accepted: 30 September 2025
Published: 24 October 2025

**Citation:** To be added by editorial staff during production.



## 1. Introduction

Studies worldwide have indicated that the global climate has resulted in changes in temperature and rainfall patterns, with many areas experiencing increasing global air temperatures. These projections are expected to continue to increase over the next 90 years in many parts of the world, as evidenced by global climate projection models (GCMs) (de Oliveira-Júnior *et al.*, 2025; Liu *et al.*, 2013; Sakellariou *et al.*, 2024; Shrestha *et al.*, 2020) This could result in a lower reduction of water supplies from increased evaporation rates, as evidenced by rising temperatures (Liu *et al.*, 2013; Sakellariou *et al.*, 2024). In addition, ocean-atmosphere projections predict that wetter regions will become wetter and drier regions will become drier (Shrestha *et al.*, 2020). Research on multiple climate processes has theoretically become socially and economically valuable. Drought is a continuous and temporary state of precipitation deficit, leading to a

**Citation:** Araya, V., Mbuh, M., Vandeberg, G., & VanLooy, J. (2025). Spatial and temporal assessment of meteorological drought using the standardized precipitation index (SPI) and its effect on crop yield over the Corn Belt region of the United States from 2000 to 2023. *Journal of Earth Observation and Geospatial Applications, 1*(1), 108–128. DOI: https://doi.org/10.65372/8h4pbf47

reduction in water supplies, encompassing a larger area and extended period over time (Tsiros *et al.*, 2020). Drought has drawn the attention of environmentalists, meteorologists, hydrologists, geologists, and agricultural scientists, as it is recognized as an environmental hazard (Mishra & Singh, 2010). As the climate changes, drought will challenge and amplify societal demands due to water stress, food insecurity, and, most critically, impacting national economies. In population growth, industry, energy, and agriculture sectors, water availability has often exceeded demand in many regions worldwide (Liu *et al.*, 2013; Mishra & Singh, 2010). Drought affects each of these sectors globally. The impacts of drought are highly synchronized across society, the environment, and the economy (Meresa *et al.*, 2023; Tsiros *et al.*, 2020). As a result, research indicates that climate variability will likely increase hydrological and meteorological droughts shortly *(*Meresa *et al.*, 2023). Moreover, climate change has influenced drought and precipitation events, leading to demands in agriculture, livestock practices, and excessive runoff, which is likely to occur in the future. As the severity and frequency of droughts increase, mitigation and adaptation strategies will be essential to support economic stability by ensuring adequate water supply during future droughts (Shiru *et al.*, 2019).

The frequency and severity of drought have increased across many regions worldwide (Sharafati *et al.*, 2020). Severe drought strongly influences the carbon cycle over lush climates such as tropical rainforests. For example, if the Amazon climate experiences more severe droughts under the influence of warming temperatures, it would potentially shift the Amazon climate into a new climate phase. Many portions of southeast Amazonia could be replaced by Savanna-like climates, influencing drier and warmer climates. Furthermore, some models suggest that there may be an increase in air temperature, which may influence increased carbon emissions, further accelerate forest degradation, and result in significant losses of carbon stocks (Duffy *et al.*, 2015). Further north, in the United States, there has been an increase in the severity and frequency of drought, particularly in the southwest United States, at the start of the 21$^{st}$ century. States impacted include Arizona, California, Colorado, New Mexico, and Utah. In spring 2022, Lake Mead and Lake Powell experienced their lowest levels. These impacts have led to landscape and ecosystem aridification. Furthermore, (Wahl *et al.*, 2022) presented that climate simulations have projected wetter climates in the northern latitudes, while southern latitudes in the subtropical regions will become drier (i.e., American Southwest). However, the exact locality for areas receiving more or less precipitation is uncertain.

Between 2000 and 2018, the United States experienced growing demand for agricultural output including both crop yields and livestock production, which has been accompanied by a decline in overall agricultural losses. These agricultural losses are related to a loss in crop production and profitability, especially in drought stricken regions like the southwest and Midwest. In the United States, the first 18 years of the 21$^{st}$ century have witnessed crop yield demand and livestock leading to reduced agricultural losses. This assessment shows crop loss has yielded over a billion dollars, with an adjusted average loss of 6.97 billion dollars and 26 heat-related deaths yearly (Leeper *et al.*, 2022). From 1989–2009, the loss contributed to 17.33 billion dollars worldwide, while the average annual loss experienced an increase of 23.125 billion dollars, far exceeding the costliest disaster of any other meteorological disaster (Wang *et al.*, 2022). From these projections, droughts are expected to become more prolonged, frequent, and severe (Li *et al.*, 2020; Shrestha *et al.*, 2020). Understanding drought characteristics is essential as it provides key information for forecasting and identifying drought. Strategies and procedures are developed to allow policy makers and stakeholders to adapt practices for resilience. This has further aided the community to learn practices to further building preparedness and response efforts to climate change. (Li *et al.*, 2020). Successful mitigation strategies and planning can be organized through best practices of interactions and coordination between local, state, regional, and national stakeholders. Specifically, these entities can provide mitigation and adaptation strategies based on historical drought (Leeper *et al.*, 2022). A drought is a non-preventable hazard, but drought resilience strategies can be implemented in response to drought hazards. The spatial and temporal characteristics are crucial for managing drought impacts and risks. Drought is a spatio-temporal process commonly characterized by its duration, intensity, and spatial extent on a regional scale (Hosseini *et al.*, 2021). Communities can practice resilience and preparedness by understanding a drought's origin, evolution, and behavior, which influence a community's economic development and well-being. Drought is linked to the deficit and decline in rainfall in a given time sequence of a season or year, and can occur in both low or high-rainfall regions (Mishra & Singh, 2010; Wilhite & Glantz, 1985). Drought is a widespread climatic event that can negatively impact agriculture productivity (cropland and rangeland) and ecological biodiversity which can lead to food insecurity by reduced surface and ground water supply used for hydropower and irrigation (Meresa *et al.*, 2023). Reduced water supply also interferes recreational water use affecting many economic and social activities (Mishra & Singh, 2010). The impacts of drought are most significant in water-stressed communities. Drought's implications regarding water quality, human health, and

critical infrastructure are less understood, which can result in indirect societal effects such as loss of electricity or industrial cooling. These communities are likely to become more vulnerable as populations in water-scarce environments grow, and the demand for water from agriculture, energy, and industry rises (Leeper *et al.*, 2022).

The Midwest is home to an agriculturally intense region that is home to one of the most essential crop commodities in the world, corn. Drought has been increasing over many parts of the world, including the United States. Understanding drought impacts on a region, such as the Corn Belt, is essential as it identifies the spatial and temporal assessment of drought, allowing this research to fill in the gap for understanding drought and its influence on crop yield. Drought is difficult to quantify, which can lead to uncertainty. Furthermore, drought is highly complex and may vary from region to region. And while one area within the region may be experiencing drought, another area may not experience drought at all. Even so, many communities have their own holistic approach for identifying drought impacts related to the demand of resources and its impact on the economy. Numerous drought indices have been developed to account for this uncertainty using rainfall, snowpack, streamflow, and other water supply indicators to provide comprehensive picture (Liu *et al.*, 2013). For example, the standardized precipitation index (SPI) and the standardized precipitation evapotranspiration index (SPEI) are excellent indices for identifying meteorological drought. (Acharki *et al.*, 2023; Li *et al.*, 2020; Stagge *et al.*, 2015). In addition, there are other remote sensing derived indices including enhanced vegetation index (EVI), evaporative stress index (ESI), normalized difference vegetation index (NDVI), vegetation condition index (VCI), temperature condition index (TCI), vegetation drought response index (VegDRI), vegetation health index (VHI), normalized difference water index (NDWI), land surface water index (LSWI), as well as soil adjusted vegetation index (SAVI), Palmer drought severity index (PDSI), standardized anomaly index (SAI), soil moisture anomaly (SMA), Palmer Z Index, aridity index (AI), and combined drought indicator (CDI) (Acharki *et al.*, 2023; Ayugi *et al.*, 2022). Monitoring meteorological drought has also been done using the PDSI , SPI, and SPEI (Sharafati *et al.*, 2020; Sun *et al.*, 2023). Some indices present unique strategies over other indices. In this study, we evaluate the processes of precipitation regimes and drought severity using the Standardized Precipitation Index of the Midwest Corn Belt Region, USA. This index can help us understand the effects of wet and dry regimes across different climate zones within a region. This index can also help us understand how these drought conditions impact one of the world's most populous crops (corn and soybeans) by presenting patterns and trends related explicitly to crop yield and production within the corn belt region, as will be assessed by this index. The study will also aid us in understanding the relevance of these impacts from the beginning of the 21st century to the most recent period of the climate record. Together, this research can aid in developing mitigation and adaptation plans designed for these agricultural communities in preparation for future drought impacts.

# 2. Study Area and Methods

## *2.1. Study Area*

The Midwest Corn Belt is located along the heartland of the United States, extending from the central and northern Great Plains into the Upper Midwest (Ort & Long, 2014; Panagopoulos *et al.*, 2015; Suyker & Verma, 2012) (Figure 1). This region can be described through the five different physiographic regions from west to east: the Great Plains, Central Lowlands, the Ozark, and the Driftless Area. The Corn Belt is defined as the region from the Great Plains stretching eastward towards the Central Lowlands that intersects the Ozark to the south and Driftless Areas to the north. The remainder of the provinces to the east are along the southern and eastern portions of the region, making up the northern portions of the Ohio River Valley: Ozark Plateaus, Coastal Plain, Interior Low Plateaus, and Appalachian Plateaus (Fenneman, 1917). Ten states define the Midwest Corn Belt. These include the states of North Dakota, South Dakota, Nebraska, Iowa, Minnesota, Wisconsin, Illinois, Indiana, Michigan, and Ohio. The study area can be divided into two sub-regions: the Eastern Corn Belt and the Western Corn Belt. The Eastern Corn Belt comprises Wisconsin, Illinois, Indiana, Michigan, and Ohio (Auch *et al.*, 2013). The Western Corn Belt comprises North Dakota, South Dakota, Nebraska, Iowa, and Minnesota. Two major river systems divide the region, tangent to one another, known as the Mississippi River and the Ohio River. The headwaters of the Mississippi River are located in Minnesota, and the Illinois flows southward towards Iowa and Illinois. Further south, the Ohio River meets the Mississippi River in Illinois and flows eastward towards southern Ohio. Interestingly, this region is native to the provinces that make up the valley of the Ohio River in the Eastern Corn Belt (Figure 1).

In the Western Corn Belt, the climate of the Great Plains is assessed by its geographic position within North America. Precipitation decreases drastically from southeast to northwest. Annual precipitation ranges from more than 32 inches in southeast Iowa to less than 16 inches in western portions of North Dakota. Annual temperature extremes show the January average temperature ranges from −5 degrees Fahrenheit in Northwest Dakota to 15 degrees Fahrenheit in southeast Nebraska and southern Iowa. Normal daily maximum temperatures in July range from values more than 90 degrees Fahrenheit in southern portions of Nebraska to around 70 degrees Fahrenheit in northeast Minnesota (Rosenberg, 1987). In the Eastern Corn Belt, the climate is maintained by factors including latitude, continental location, large-scale circulation, and the presence of the Great Lakes. Average annual temperatures from 1980–2010 range from 40 degrees Fahrenheit in the North Shore and Upper Peninsula to 55 degrees Fahrenheit in southern Illinois and Indiana. Average winter temperatures from DJF range from 10 degrees Fahrenheit in northern Wisconsin to 30 degrees Fahrenheit in southern Illinois, Indiana, and Ohio. DJF refers to climatological season winter months of December, January, February (Chen *et al.*, 2024). Total annual precipitation ranges from 25 inches in the north of Michigan to as much as 45 inches in the southern portions of Illinois, Indiana, and Ohio. Summertime precipitation in JJA has annual maximum rainfall from the western portions of Wisconsin and minimum precipitation along Michigan's upper peninsula. Refer to Figure 1 below.

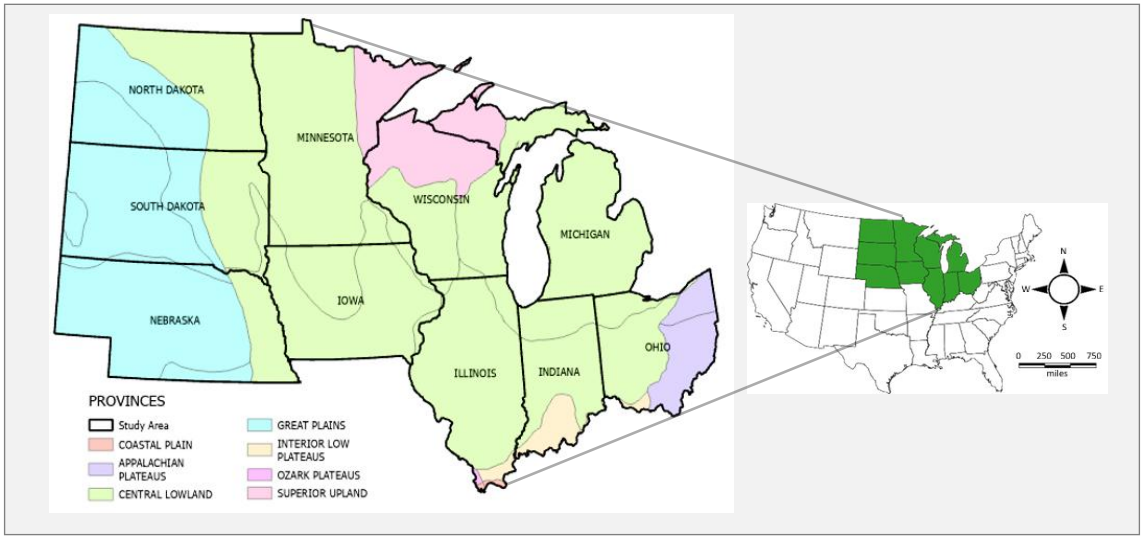


**Figure 1.** Study area. Corn Belt Region Provinces. The map shows provinces from west to east along the Western and Eastern Corn Belt; Great Plains, Coastal Lowland, Superior Upland, Ozark Plateau, Coastal Plain, Interior Low Plateaus, and Appalachian Plateaus. Credit by Esri.

## *2.2. Data*

The data used for this study include CHIRPS (Climate Hazards Group InfraRed Precipitation with Station Data) which provides precipitation data from 1981 such as UCSB-CHG/CHIRPS/DAILY (or monthly), GridMET Drought dataset, cropland cover data, yield data, and crop condition/progress monitoring datasets (Funk *et al.*, 2015). The CHIRPS dataset was adopted by the U.S. Geological Survey (USGS) and the University of California at Santa Barbara to provide global precipitation at high spatial resolutions. These were set at resolutions of 0.05 degrees and 0.25 degrees, providing precipitation data from 1981 to the present (de Oliveira-Júnior *et al.*, 2021; Du *et al.*, 2024; López-Bermeo *et al.*, 2022). Cropland cover data was used to analyze and create the maps for cropland cover for the years in the climate record (Han *et al.*, 2012). Yield data from USDA NASS crop statistics were used to aid in calculating cropland cover for the crop types designed to quantify measured crop types in Bushels per hectare over the entire region. Crop condition/progress was used to create a condition progress table to indicate the percentage of crop cover compared to drought/wetness years (Boryan *et al.*, 2011). All the data used for this research were accessible via Google Earth Engine.

## *2.3. Methods*

The standardized precipitation index is widely used to assess meteorological drought on various timescales. This precipitation data is typically distributed as a Pearson Type III or gamma distribution and is lastly categorized into a normal distribution as this is demonstrated in Eqs 7&8 (Schneider *et al.*, 2013). We demonstrate how the SPI equation works in the following paragraph.

The first step in presenting the calculation of the SPI is to assess a probability density function that describes the long-term series of observations (Eq. 1–4). Second, the cumulative probability of an observed precipitation amount is computed once the distribution is examined. The inverse normal (Gaussian function) is then processed to the likelihood, which defines the SPI. The values of SPI are positive (negative) for greater (less) than the median precipitation. The departure from zero results in a probability of the severity of wetness or aridity that can be used for risk assessment. Following these steps from (Guttman, 1998; Guttman, 1999), the gamma distribution as in (Eq.1) (defined by (Angelidis *et al.*, 2012; Bouaziz *et al.*, 2021; Liu *et al.*, 2021; Lloyd-Hughes & Saunders, 2002; Sönmez *et al.*, 2005) can be described as follows:

$$g(x) = \frac{1}{\beta^{\alpha}\Gamma(\alpha)} x^{\alpha-1} e^{-x/\beta} \quad (1)$$

$\alpha > 0$ $\alpha$ is a shape parameter.

$\beta > 0$ $\beta$ is a scale parameter.

$x > 0$ x is the precipitation amount.

$\Gamma(\alpha) = \lim_{n\to\infty} \prod_{v=0}^{n-1} \frac{n! n^{y-1}}{y+v} \equiv \int_0^{\infty} y^{\alpha-1} e^{-y}\, dy$ $\Gamma(\alpha)$ is the gamma function.

where $G(x)$ It is the average likelihood of the data series being converted into an incomplete gamma distribution. According to (Lloyd-Hughes & Saunders, 2002), $\Gamma(\alpha)$ It is a unique arithmetic approach that expands on the implication leading to the final equation.. To fit the distribution, the parameters of $\alpha$ and $\beta$ need to be estimated. Therefore, these parameters are calculated for each station, for each time scale of interest (3 months, 12 months, 48 months, etc.), and for each month of the year. This process can be examined as follows:

$$\alpha = \frac{1}{4A}\left(1 + \sqrt{1 + \frac{4A}{3}}\right) \quad (2)$$

$$\beta = \frac{\bar{x}}{\hat{\alpha}} \quad (3)$$

For n observations, we have

$$A = \ln(\bar{x}) - \frac{\sum \ln(x)}{n}. \quad (4)$$

Integrating the probability distribution function (Eq 5) concerning x and inserting the estimates of $\alpha$ and $\beta$ gives an expression for the cumulative probability G(x) for an observed amount of precipitation occurring for a given month and time scale.

$$G(x) = \int_0^x g(x)\, dx = \frac{1}{\hat{\beta}^{\hat{\alpha}}\Gamma(\hat{\alpha})} \int_0^x x^{\hat{\alpha}} e^{-x/\hat{\beta}}\, dx \quad (5)$$

which can be expressed as the incomplete Gamma function. As the gamma function is undefined at x = 0 and a precipitation distribution may contain zeros, the cumulative probability becomes:

$$H(x) = q + (1 - q)G(x) \quad (6)$$

Statistically, $q = P(x = 0) > 0$ where $P(x = 0)$ It is the probability of zero precipitation (Eq 6). The cumulative probability distribution is converted into the standard normal distribution to yield the SPI (Eqs 9-11). Moreover, it can be transformed into the standard normal random variable Z with mean zero and variance

of one, which is the value of the SPI. The Z or SPI value in Eq 7&8 is more easily obtained computationally using an approximation designed by (Bouaziz *et al.*, 2021; Lloyd-Hughes & Saunders, 2002), which converts the cumulative probability to a standard normal random variable Z as follows:

$$Z = SPI = -(t - \frac{t - C_0 + C_1 t + C_2 t^2}{1 + d_1 t + d_2 t^2 + d_3 t^3}) \quad \text{for } 0 < H(x) \leq 0.5 \tag{7}$$

$$Z = SPI = +(t - \frac{t - C_0 + C_1 t + C_2 t^2}{1 + d_1 t + d_2 t^2 + d_3 t^3}) \quad \text{for } 0.5 < H(x) < 1 \tag{8}$$

Where $t$ is given as

$$t = \sqrt{\ln\left[\frac{1}{(H(x))^2}\right]} \quad \text{for } 0 < H(x) \leq 0.5 \tag{9}$$

$$t = \sqrt{\ln\left[\frac{1}{(1 - H(x))^2}\right]} \quad \text{for } 0.5 < H(x) < 1 \tag{10}$$

$$C_0 = 2.515517 \qquad C_1 = 0.802853 \qquad C_2 = 0.010328 \tag{11}$$

$$d_1 = 1.432788 \qquad d_2 = 0.189269 \qquad d_3 = 0.001308$$

For crop yield, the data was calculated to represent bushels of total production as the first method for the analysis. First, the raster layer is 30 meters by 30 meters in spatial resolution. The total area in resolution is 900 $m^2$. To find the location in acres, square meters were converted to acres to get the total area in acres. Lastly, the total area (acres) and crop yield data were converted to bushels per acre to get the overall production in bushels per acre using the equation below. These calculation steps were applied for Corn and soybean crops individually, and then all crop types combined. The resolution of the dataset was 30 m. The total area of the dataset was 900 m. The total length of the pixel was given in meters ($m$). The total resolution area was multiplied by the pixel length to get the total area in acres.

- Resolution = 30 m
- Area
  - 30 m * 30 m = 900 $m^2$
  - Count * 900 $m^2$

Next, the total area is converted from $m^2$ to acres as follows:

- Area ($Ac$)
  - Area $m^2$ * 0.000247 $\frac{Ac}{m^2}$
- Total production ($BU$)
  - Area ($Ac$) * Yield * ($\frac{BU}{Ac}$) = Total Production ($BU$)

The first step introduces the resolution of the dataset that is represented in $m^2$. The second calculation process represented three different quantities of crops. While the above equation indicates the calculation for total production ($BU$), the analysis was conducted in a modified format. The first and second crop types in this research are corn and soybeans. The last quantity is the sum of all crop types, in addition to corn and soybeans, that make up the entire Corn Belt. The overall production was represented in finalized units. $m^2$. Corn, soybeans, and all crops were categorized accordingly, placing each in a pie chart for each year to represent these quantities. Crop condition and crop progress were the second methods used for the analysis. Even though this step is part of the calculation process, it will not be treated as the calculation. In this procedure, there are three rows. The first graph shows good, excellent crop progress and conditions (Figure 2 on next page). The second graph represents the percentage or type in each condition category (excellent, good, fair, poor and very poor). The third graph represents the progress percentage (planted, emerged, silking, dented, matured, etc.). For this research, we will stick to the first row. The condition progress is recorded for each type of crop. The colored line represents the time series for the first five years. The lines run from April to October. At the end of each line, the crop progress is processed in a table. On the right side is a list of all

crops grown from January to December. As observed, all crops are harvested from May to September, as denoted in Figure 2b. The first part of the figure is the crop time series. The second part is seasonal crops (Figure 2).

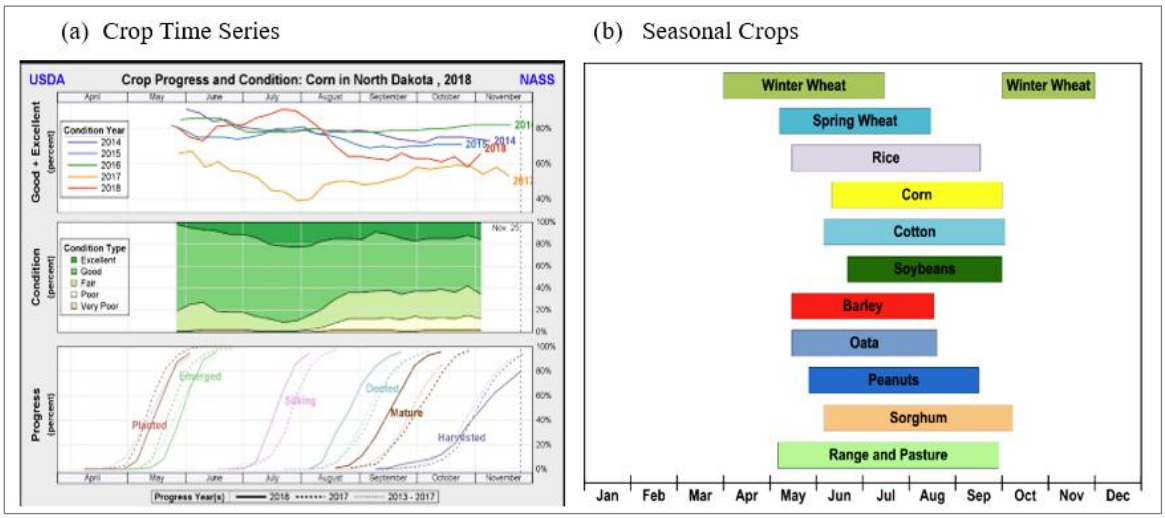


**Figure 2.** (a) Crop progress and condition grown in ND, 2018, of condition year (1st graph), percent by condition type (2nd graph), and average. Plant growth stage across the growing period (3rd graph) and (b) Seasonal crops of annual variation of crop types grown in the U.S. Credit by USDA.

## 3. Results and Discussion

This study provides a detailed assessment of drought variability across the Corn Belt, examining its spatial and temporal patterns over more than twenty years. Using the standardized precipitation index, clear distinctions are made between periods of extreme, severe, moderate, and non-significant drought. These classifications reveal how dry and wet conditions shift over time and also show how drought severity directly affected crop yields for corn and soybeans throughout the region. The analysis shows that drought years often led to significant drops in crop productivity, while years without drought generally resulted in higher-than-average yields. The results are discussed in two parts. Section one discusses the relationship between wet and dry conditions over the region using the SPI index (Mishra & Singh, 2010; Wilhite & Glantz, 1985). Section two discusses the wet and dry conditions and their influence on crop yield (Green *et al.*, 2018; Mishra & Singh, 2010; Wilhite & Glantz, 1985). The results can be discussed using the drought classification: extreme, severe, moderate and no significant drought. All five of these classes are distributed through the years over the entire climate record. The second section discusses these classifications using the cropland cover and crop quantities (crop yield assessment) and crop harvest and progress affected directly by these drought classifications. For assessing crop yield impacted by drought, values from crop progress and condition (Figure 2a) were interpolated onto a table represented in 3.2 of this chapter. Threshold levels were used to assess each crop yield class impacted by each classification of drought. The following thresholds are defined as follows: extreme drought (35 percent or less), severe drought (40 percent or less), and moderate drought (45 percent or less). Non-significant drought differs. It is used to describe much of the region, including all states, that was under an area that indicated no drought. Therefore, to make the classification more specific and consistent with the results, threshold levels were defined as above average (60–79 percent) and well above average (80 percent or greater). These two thresholds were defined as productive (above average) or extremely productive (well above average) thresholds. These thresholds were used based on the statistical probability at which these values corresponded to on each drought classification.

### *3.1. Relationships Between Wet and Dry Conditions Over the Corn Belt Region Over 20 Years*

In 2012, major drought coverage extended in the Eastern and Western Corn Belt regions. Widespread

extreme dry conditions extended from Nebraska and South Dakota, spreading eastward to Ohio and Michigan (Figure 3a). Widespread extreme conditions dominated most of these states, with Nebraska and South Dakota representing a much larger area of widespread extreme dryness (Shrestha *et al.*, 2020). In the East Corn Belt, widespread extremely dry conditions were observed in Wisconsin, Indiana, and portions of Ohio (Auch *et al.*, 2013; Mishra & Singh, 2010; Wilhite & Glantz, 1985). Portions of Illinois and Michigan also indicated extreme conditions, but these conditions were not as widespread as in these other states (Figure 3).

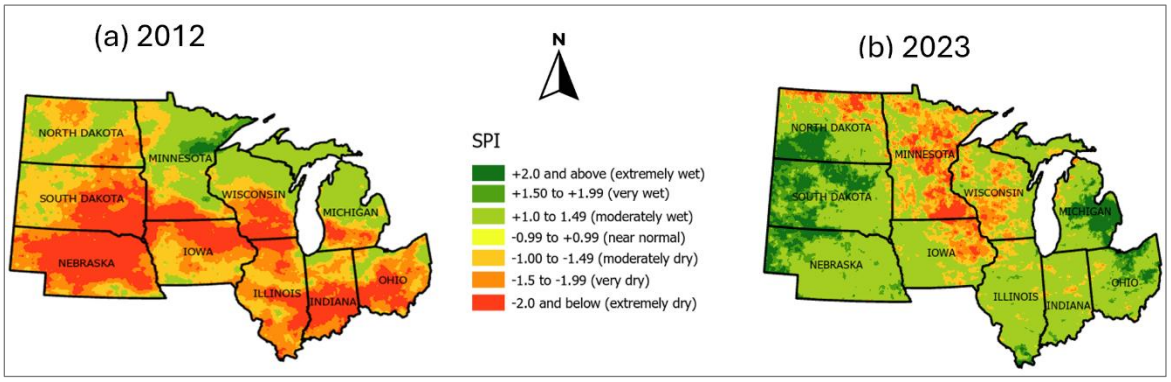


**Figure 3.** Extreme dryness (−2.0 and below) over the entire corn belt; (a) 2012; (b) 2023. Figure representing the region that represented extreme dryness during the years of extreme drought. Displayed using the SPI index.

In 2023, numerous pockets of severe to extreme dryness were observed along a diagonal extending from North Dakota into sections of Iowa and Wisconsin (Ort & Long, 2014; Panagopoulos *et al.*, 2015; Suyker & Verma, 2012) (Figure 3b). Many states indicated frequent pockets of these drought episodes, especially in Minnesota, where severe to extreme dry pockets were present in numerous places across the region (Meresa *et al.*, 2023).

The intensity and coverage of severe droughts were the greatest, especially in 2002 and 2006, along the Western Corn Belt. Despite severe conditions in the eastern states in 2011, 2002, and 2006 experienced numerous and widespread impacts. Impacts were mainly along the west and east corn belt in 2002, with 2006 indicating severe impacts along the Dakotas and into Minnesota.

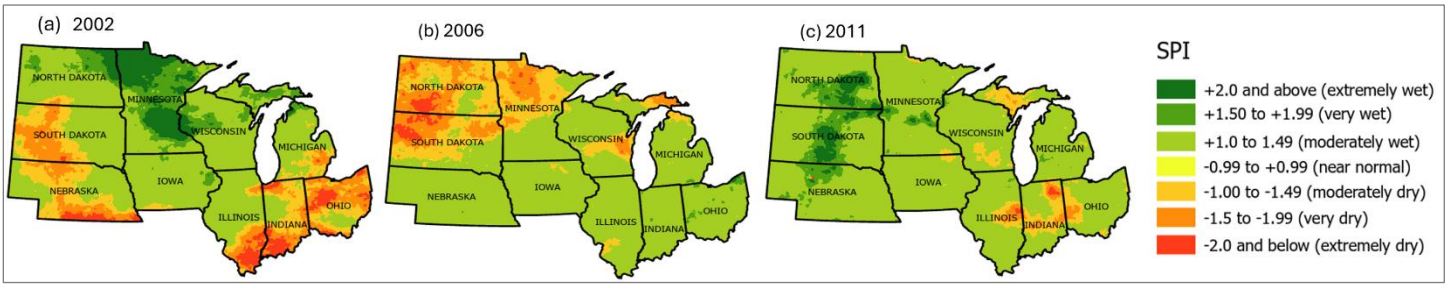


**Figure 4.** Severe dryness (−1.5 to −1.99) over the entire corn belt; (a) 2002, (b) 2006, (c) 2011. Figure representing the region that represented severe dryness during the years of severe drought. Displayed using the SPI index.

In 2002, drought conditions were observed from the North Dakota border and into South Dakota, stretching southward towards Nebraska (Figure 4a). Moderately arid conditions were along the northern portion of this boundary, especially in South Dakota (Meresa *et al.*, 2023; Mishra & Singh, 2010). Going southward, conditions worsened from severe to extreme, especially along the Nebraska border (Shrestha *et al.,* 2020).

In 2006, severe to extreme dryness was observed, especially along the western portions of the Dakotas, extending into Minnesota along the northern portion of the state (Figure 4b). Coverage was widespread along this region of the west belt, especially along the western sections of the Dakotas. Here, severe dryness was numerous with some sections indicating extreme dryness. In moderate drought years, 2013 and 2021 experienced numerous and widespread coverage of severe drought throughout most of the region *(*Meresa *et*

*al.*, 2023; Mishra & Singh, 2010; Wilhite & Glantz, 1985). While 2013 was the greatest drought year recovering from the 2012 major drought, impacts were still widespread in coverage and intensity throughout the entire region, especially along the southern corn states (Auch *et al.*, 2013; Meresa *et al.*, 2023). Drought coverage extended from Nebraska and stretched into Indiana (Figure 5b). Conditions of severe dryness, with some pockets of extreme dryness, were observed, especially in Illinois (Figure 5).

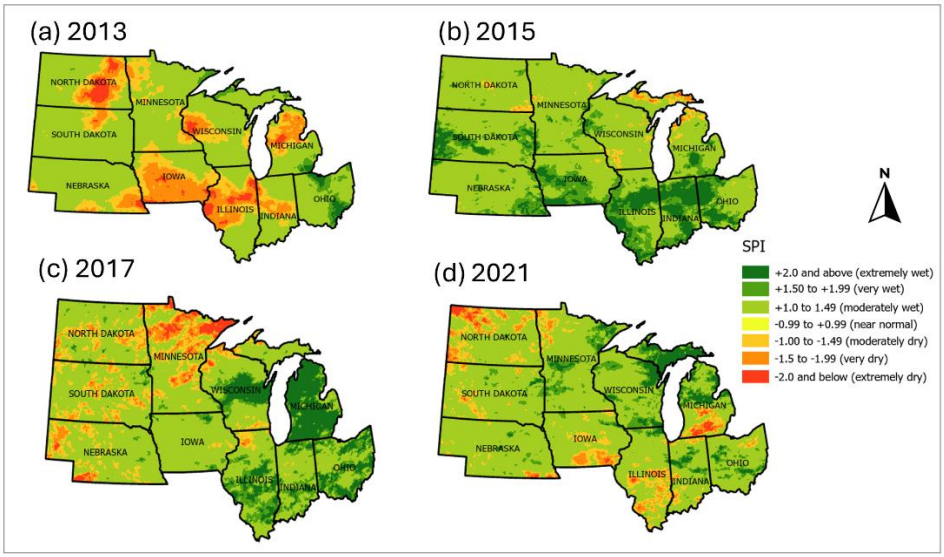


**Figure 5.** Moderate dryness (−1.00 to −1.49) over the entire corn belt. (a)2013, (b) 2015, (c) 2017, (d) 2021 Figure representing the region that represented moderate dryness during the years of moderate drought. Displayed using the SPI index.

The year 2021 indicated drought impacts mainly along the west corn belt, but in numerous pockets, with drought increasing northeastward towards the Superior Northland, sustaining the most significant impacts (Leeper *et al.*, 2022; Mishra & Singh, 2010; Sakellariou *et al.*, 2024). Moreover, while the Eastern Corn Belt indicated wetness, the Western Corn Belt showed significant dryness impacts (Figure 5d). Much of the Great Plains extending northeast to northland shore regions encompassed a greater expanse of dryness, especially near the northland shore, where more widespread dryness was observed (Shrestha *et al.*, 2020). The Great Plains experienced pockets of dryness from Nebraska to North Dakota (Ort & Long, 2014; Panagopoulos *et al.*, 2015; Suyker & Verma, 2012). Pockets were scattered throughout these states, especially towards the west. Specifically, the southwest border of Nebraska experienced patches of intense and severe impacts along this subregion of the Western Corn Belt (Auch *et al.*, 2013). Regionally, dryness increased from southwest to northeast, where much of Minnesota's north shore had the most significant impacts along the northeast corner of Lake Superior and into the border of Canada. While 2015 and 2017 indicated impacts from drought, they were not as extreme as the other years described. In 2003, much of the Western and Eastern Corn Belt exhibited moderately wet conditions despite spotty sections of drought in western sections of the Dakotas and eastern Nebraska (Figure 6a). In 2004, moderate wetness was much more widespread than in the previous year, and it was prominent in both Corn Belts (Figure 6b). Drought remained in northern sections of the region (Figure 6).

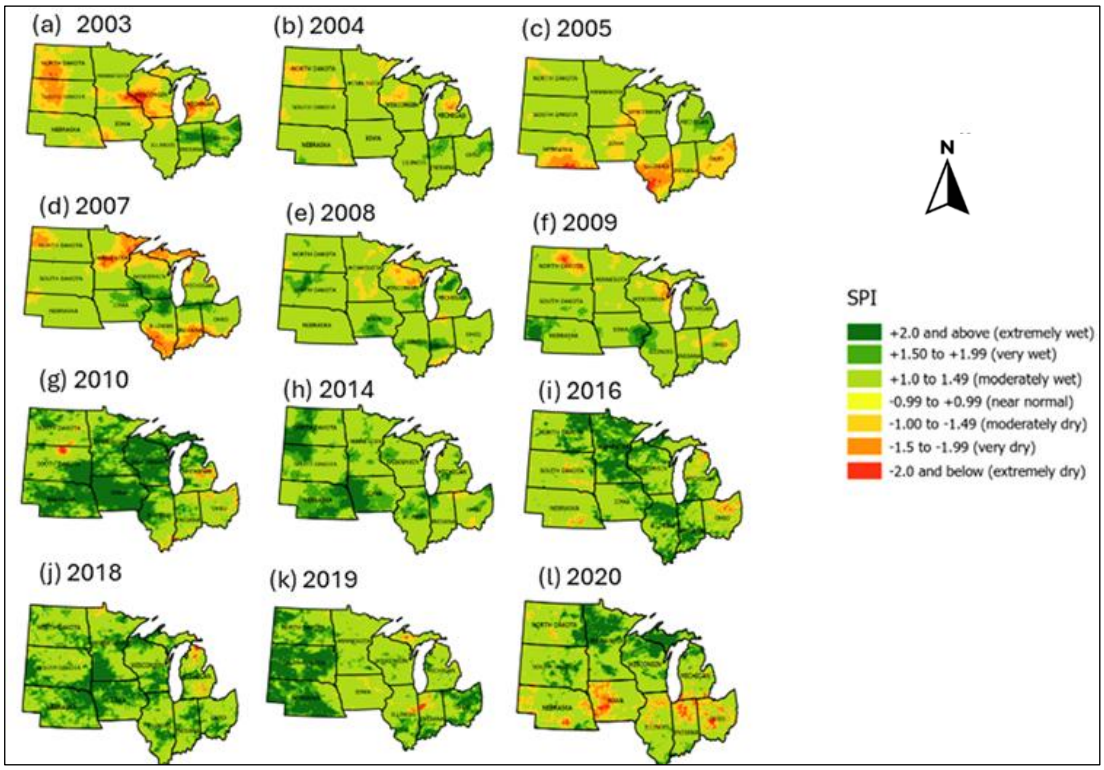


**Figure 6.** No significant drought. Near normal (–0.99 to +0.99), moderately wet (+1.0 to 1.49), very wet (+1.50 to +1.99), and extremely wet (+2.0 and above). (a) 2003; (b) 2004, (c) 2005; (d) 2007; (e) 2008; (f) 2009; (g) 2010; (h) 2014; (i) 2016; (j) 2018; (k) 2019; (l) 2020. Figure representing the region that represented near-normal to extreme wetness during the years of non-drought. Displayed using the SPI index.

In 2005, widespread moderate wetness conditions were observed along the northern half of both corn belts. Very wet conditions can be observed over eastern Michigan while southern sections of the region remained in drought (Liu *et al.*, 2013; Sakellariou *et al.*, 2024; Shrestha *et al.*, 2020). In 2007, widespread drought-free conditions were observed in the region's interior, with excessive wetness increasing towards the middle (Figure 7d). Here, a section of excessive wetness can be observed overlapping the Western and Eastern Corn Belt Regions, extending towards the eastern states of the Eastern Corn Belt Region (Auch *et al.*, 2013). In 2008, widespread drought-free conditions were observed throughout the region, especially towards the west, where drought improved along Lake Superior's northland region and the Ohio Valley (Figure 6e). Widespread wet conditions were observed along the Western Corn Belt, especially in the western states of the Great Plains. Much of the region experienced moderate to severe wet conditions along the Eastern Corn Belt. Severe wetness was along sections of southeast Wisconsin, southern sections of Illinois and Indiana, and northern Michigan. While drought conditions have shown significant improvement along Northland Superior and the Ohio Valley, widespread moderate wetness was dominant throughout the region. Overall, pockets of severe to excessive wetness were scattered throughout the region (Leeper *et al.*, 2022; Meresa *et al.*, 2023). In 2009, moderate wetness conditions dominated much of the landscape, especially the Western Corn Belt Region, where severe to extreme wetness was present along the panhandle of Nebraska and southeast sections of Iowa (Figure 6f). Drought conditions improved along the northern Great Lakes. In 2010, much of the region experienced widespread extreme wetness conditions, making it the wettest year in this drought-free group, especially along the Western Corn Belt (Meresa *et al.*, 2023; Mishra & Singh, 2010; Ort & Long, 2014; Panagopoulos *et al.*, 2015; Suyker & Verma, 2012). This pattern was extended from the southern Great Plains into the northern Great Lakes Region, putting a significant dent in the drought in this area. While the Eastern Corn Belt exhibited wet conditions, especially in the western states, this region was not as intense. Moderate wetness was the main culprit along the eastern portions of the area. While 2014 and 2016 experienced widespread wetness intensity, they were not as widespread as 2010. In 2014, much of the region experienced a drought-free year, with many areas indicating moderate wetness (Wilhite & Glantz, 1985). Severe to extreme wetness was noted along the western portion of the Dakotas and southern sections of the Western Corn Belt (Nebraska and Iowa). In 2016, both belts also experienced moderate wetness (Figure

6i). A boundary of extreme wetness was observed dividing this line, which could be extended from the Ohio Valley and into the northern Prairie Pothole region states (Ort & Long, 2014; Panagopoulos *et al.*, 2015; Suyker & Verma, 2012). This was a diagonal of intense wetness covering most of the region, which extending from North Dakota, stretching southeastward towards Illinois and Indiana. Similar to 2016, 2018, and 2019 experienced widespread moderate wetness with excessive wetness along the Great Plains into much of the Prairie Pothole states and sections of Indiana and Ohio (Auch *et al.*, 2013). Conditions were not as intense as receding years, but still indicated pockets of severe to extreme wetness along these areas (Figures 6j & 6k).

### *3.2. Impact of Drought Conditions on Crop Yield in the Region*

In the extreme drought years, corn and soybeans represented widespread distribution throughout the region, originating from North Dakota down into Nebraska and extending eastward towards Illinois, Indiana and Ohio (Brandes *et al.*, 2016; Green *et al.*, 2018; Ort & Long, 2014; Panagopoulos *et al.*, 2015; Peña-Gallardo *et al.*, 2019; Prince *et al.*, 2001; Suyker & Verma, 2012; Wilson *et al.*, 2022)(Figures 7a & 7b).

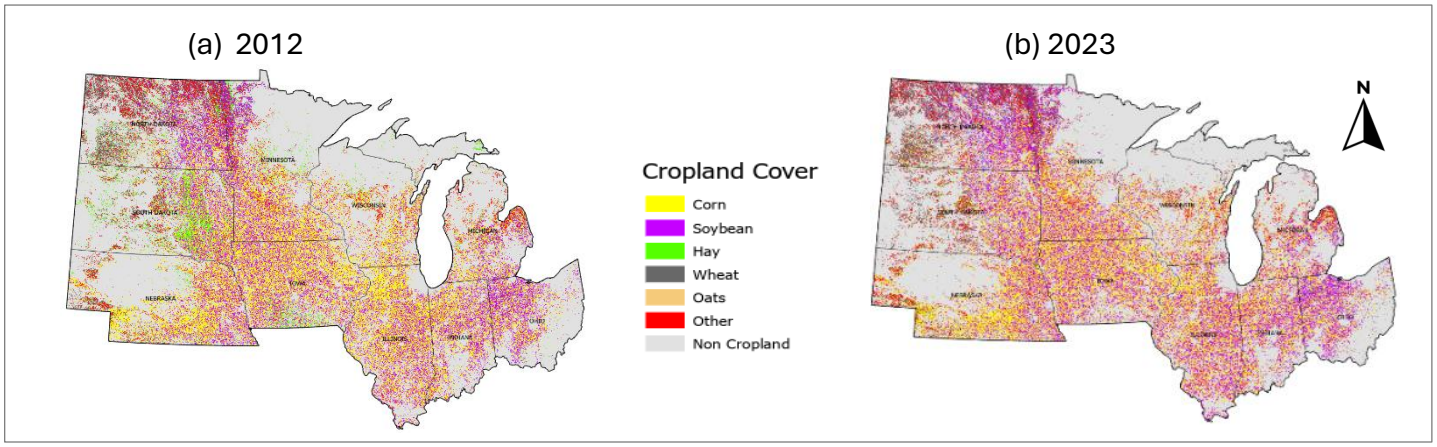


**Figure 7.** Cropland cover of extreme drought years. Figure describing corn, soybean, hay, wheat, oats, and other cropland over the Corn Belt Region. (a) 2012 crop cover, (b) 2023 crop cover. Crop cover is not a measure of drought impacts but of crop rotation, plantations, and depletion.

Regarding the drought impacts, crop yield experienced very low levels for both crops, especially for corn yield. These threshold levels as defined in introduction of this chapter most impacted the Eastern Corn Belt. Crop production and harvest of corn were low for the following states: Nebraska, Iowa, South Dakota, Illinois, Wisconsin, Indiana, Michigan, and Ohio (Green *et al.*, 2018; Liu *et al.*, 2013). Corn was exceptionally low, and the lowest crop progress was 30% or less in some states over other years, especially for Iowa, South Dakota, Illinois, Indiana, Michigan, and Ohio, with Illinois representing the lowest production and harvest (Fadhli *et al.*, 2020; Green *et al.*, 2018). As for soybeans, threshold levels were not as low, but some states indicated below threshold levels (Prince *et al.*, 2001). These states included Nebraska, South Dakota, Wisconsin, and Illinois. Nebraska represented the lowest threshold level. (Table 1). Corn and soybean quantities were less in the year, 2023 (Figure 8). While these quantities were less for this year corn still indicated a greater quantity than soybeans (Green *et al.*, 2018; Leeper *et al.*, 2022). In 2023, corn and soybean quantities were larger than in the preceding year.

**Table 1.** Crop production thresholds of extreme drought. Table 1 describes the impacts of corn and soybeans for the years impacted by extreme drought in the Corn Belt Region. The table demonstrates the impacts of drought on crop yield.

| Year | Nebraska | Iowa | South Dakota | North Dakota | Minnesota | Illinois | Wisconsin | Indiana | Michigan | Ohio |
|---|---|---|---|---|---|---|---|---|---|---|
| Corn | | | | | | | | | | |
| 2012 | 32 | 20 | 25 | 57 | 59 | 7 | 36 | 12 | 27 | 16 |
| 2023 | 51 | 51 | 48 | 57 | 40 | 55 | 53 | 68 | 47 | 87 |
| Soybean | | | | | | | | | | |
| 2012 | 23 | 32 | 27 | - | 60 | 40 | 26 | 27 | 39 | 36 |
| 2023 | 40 | 51 | 45 | - | 44 | 48 | 60 | 67 | 48 | 81 |

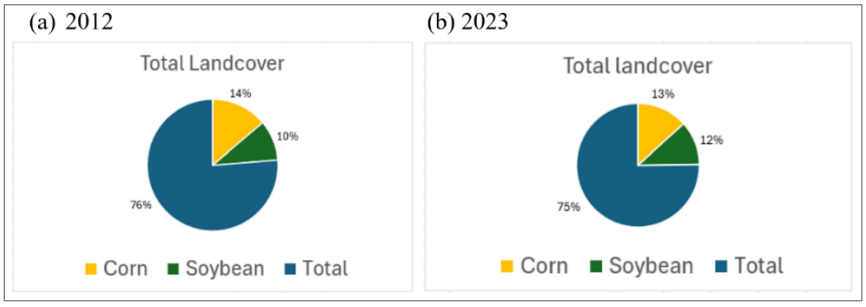


**Figure 8.** Total landcover distribution of extreme drought years. Crop quantities of corn (orange), soybean (green), and total overall crop distribution of the Corn Belt Region. Not a reflection of drought impacts. Credit by CropScape.

During the severe drought years, corn and soybeans were distributed throughout the southern states (Green *et al.*, 2018). The prevalence of crop diversity (other crops) blended in, especially during the earlier periods (2002 and 2006), but then decreased towards 2011. Oats were also introduced, especially during the beginning period (2002), and have since risen throughout the period (2006 and 2011). Soybean concentrations were also prevalent, especially in the eastern states. Crop cover is not a measure of drought impacts but of crop rotation, plantation, and depletion. (Figure 9). For drought impacts, 2011 indicated minimal impacts. And 2002 experienced the lowest yields for both crops, especially in the Eastern Corn Belt, with soybean indicating the lowest yield in Ohio of around 12%. While soybeans were also impacted, low corn yield was much more frequent for these states (Indiana and Ohio). These quantities ranged from 13–35% harvest. While 2006 and 2011 experienced low levels, they were less impactful than 2002 (Table 2).

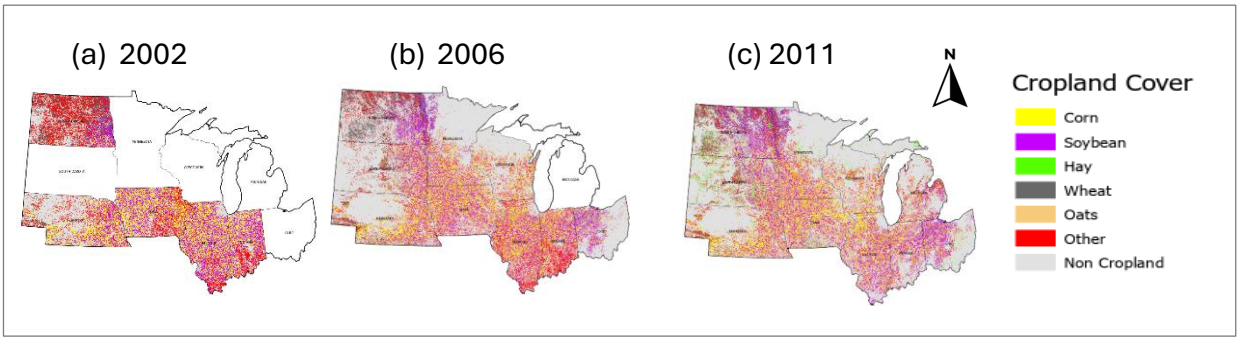


**Figure 9.** Cropland cover of severe drought years showing corn, soybean, hay, wheat, oats, and other cropland over the Corn Belt Region. (a) 2002 crop cover, (b) 2006 crop cover, and (c) 2011 crop cover.

**Table 2.** Crop production thresholds of severe drought. Table 2 describes the impacts of corn and soybeans for the years impacted by extreme drought in the Corn Belt Region. The table demonstrates the impacts of drought on crop yield in the region.

| Year | Nebraska | Iowa | South Dakota | North Dakota | Minnesota | Illinois | Wisconsin | Indiana | Michigan | Ohio |
|---|---|---|---|---|---|---|---|---|---|---|
| Corn | | | | | | | | | | |
| 2002 | 33 | 71 | 42 | 59 | 73 | 35 | 65 | 26 | 44 | 13 |
| 2006 | 57 | 73 | 32 | 36 | 68 | 73 | 62 | 72 | 71 | 72 |
| 2011 | 79 | 59 | 72 | 57 | 57 | 45 | 79 | 36 | 64 | 59 |
| Soybean | | | | | | | | | | |
| 2002 | 23 | 65 | 43 | - | 72 | 39 | 67 | 32 | 53 | 12 |
| 2006 | 62 | 75 | 50 | - | 66 | 73 | 65 | 74 | 73 | 67 |
| 2011 | 77 | 65 | 64 | - | 55 | 51 | 75 | 43 | 68 | 64 |

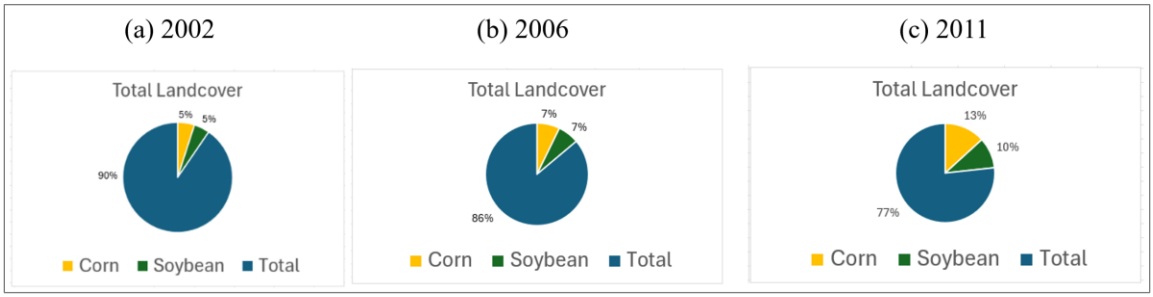


**Figure 10.** Total landcover distribution of severe drought years. Crop quantities of corn (orange), soybean (green), and total overall crop distribution of the Corn Belt Region. Not a reflection of drought impacts. Credit by CropScape.

Low crop quantities were indicative of missing data on cropland cover for these years (Figure 10). While missing data returned to normal levels, this indicated an increased production of tremendous quantities of one-quarter of the overall distribution for both crops. Overall crop cover distribution is the largest in 2002, of around seven-eighths, but then decreased to three-quarters of the distribution in 2011. In moderate drought years, corn and soybean concentrations increased throughout the severe drought years (2002, 2006, and 2011). Crop patterns remained stagnant and consistent throughout the period, with little to no change. (Figure 11).

**Table 3.** Crop production thresholds of severe drought. Table 3 describes the impacts of corn and soybeans for the years impacted by severe drought in the Corn Belt Region. Table demonstrates the impacts of drought on crop yield in the region.

| Year | Nebraska | Iowa | South Dakota | North Dakota | Minnesota | Illinois | Wisconsin | Indiana | Michigan | Ohio |
|---|---|---|---|---|---|---|---|---|---|---|
| Corn | | | | | | | | | | |
| 2013 | 68 | 49 | 65 | 51 | 59 | 67 | 47 | 73 | 68 | 84 |
| 2015 | 76 | 84 | 80 | 71 | 88 | 56 | 79 | 48 | 72 | 52 |
| 2017 | 64 | 66 | 48 | 54 | 82 | 63 | 71 | 59 | 56 | 69 |
| 2021 | 71 | 62 | 21 | 16 | 37 | 70 | 72 | 70 | 73 | 79 |
| Soybean | | | | | | | | | | |
| 2013 | 69 | 42 | 54 | - | 55 | 63 | 43 | 68 | 58 | 72 |
| 2015 | 74 | 77 | 78 | - | 83 | 60 | 80 | 51 | 66 | 53 |
| 2017 | 64 | 64 | 53 | - | 69 | 60 | 74 | 58 | 43 | 58 |
| 2021 | 74 | 63 | 24 | - | 36 | 72 | 73 | 69 | 63 | 67 |

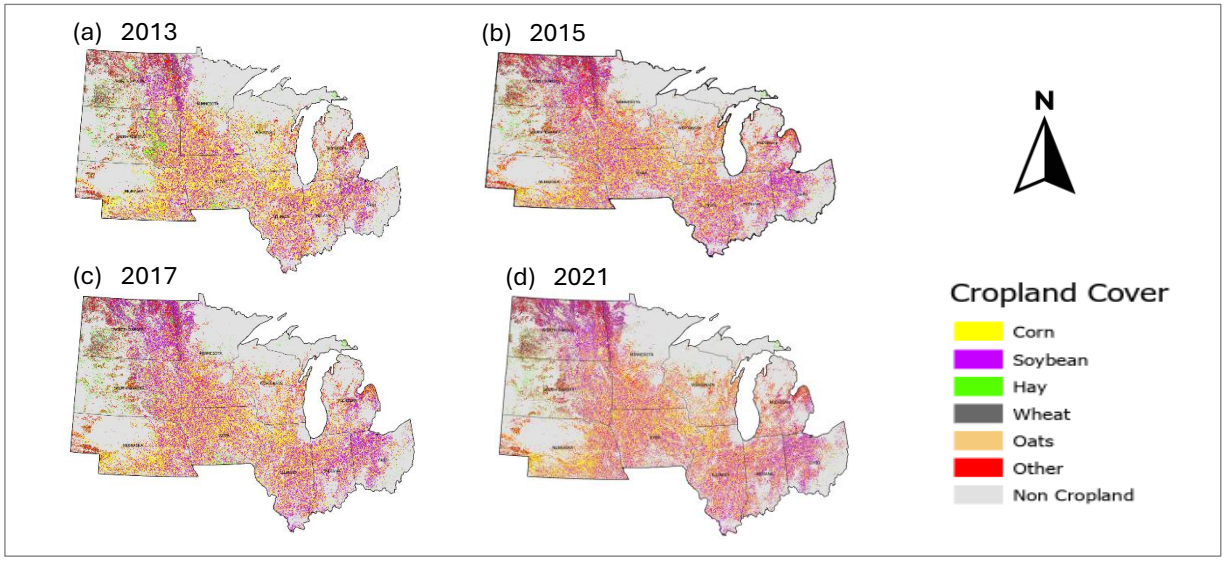


**Figure 11.** Cropland cover of moderate drought years. Figure describing corn, soybean, hay, wheat, oats, and other cropland over the Corn Belt Region. (a) 2012 crop cover, (b) 2023 crop cover. Crop cover is not a measure of drought impacts but of crop rotation, plantations, and depletion.

For drought impacts, 2021 indicated the most impactful crop yield impacts for both crops along the Western Corn Belt, with both crops severely impacted. Moreover, the Western Corn Belt was most impacted. The threshold level fell within severe limits for corn yield, especially in the west. Severe threshold levels were reported for South Dakota, North Dakota, and Minnesota. North Dakota indicated the lowest threshold levels. For soybeans, impacts were not as low but still within severe limits, with South Dakota indicating the lowest level. While earlier years exhibited drought conditions throughout the region, they did not experience severe threshold levels and instead witnessed unusually productive levels, especially in 2015 (Table 4). Crop quantities showed that in 2013 and 2015, less than one-quarter of the distribution was displayed as corn and soybean cover. The years 2017 and 2021 indicated a gradual increase in corn and soybean quantities. Overall crop distribution remained consistent with little to no change in distribution throughout the period. (Figure 12).

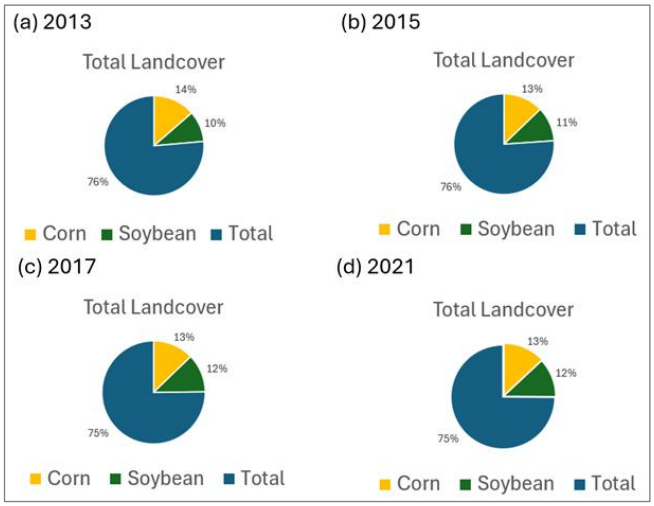


**Figure 12.** Total landcover distribution of moderate drought year. Crop quantities of corn (orange), soybean (green), and total overall crop distribution of the Corn Belt Region. Not a reflection of drought impacts.

During non-drought years, corn and soybeans started with an early period (2003–2005) of crop diversity blended with corn and soybean distribution but then decreased with more cropland cover of corn and soybean

concentrations after 2007. Crop diversity was prevalent but was more observable in the southern sections of Illinois and Indiana, along with Wisconsin and Michigan. (Figure 13). In 2009 and 2010, much of the landscape was unchanged (Figures 13f & 13g). New plantations of hay were added to sections of eastern South Dakota in 2010. From here, the crop was a dominant practice along the corn/soybean belt areas. It spread to other locations, such as North Dakota, Iowa, and Nebraska. Corn and soybean distribution was distributed from the Western Corn Belt from North Dakota down into Nebraska, extending eastward towards the east belt states, presenting permanent land cover practices throughout the period (Auch *et al.*, 2013). While crop rotations became prominent in this region, crop diversity decreased (after 2005), preserving more corn and soybean concentrations (after 2007) and blending other crops such as hay and oats (after 2010). In terms of non-drought impacts, above to well above average threshold levels were indicated, especially during the middle period, where numerous conditions indicated the wealthiest production. Both 2010 and 2016 experienced the highest productivity of these conditions, where numerous reports indicated well above average production throughout the region (Leeper *et al.*, 2022; Meresa *et al.*, 2023; Mishra & Singh, 2010). For both crops, Nebraska, North Dakota, Minnesota, and Wisconsin all experienced maximum thresholds. Minnesota indicated the most significant levels of production. Above to well-above-average conditions were represented throughout the region, especially corn yield, which indicated numerous maximums in 2010. Iowa, North Dakota, Minnesota, and Wisconsin were among the wealthiest productive states for both crops in 2016. While both crops were among their maximum and most productive harvest of any other year, corn yield indicated the greatest productivity, making it one of the most valuable crops harvested in the region (Green *et al.*, 2018; Ort & Long, 2014; Panagopoulos *et al.*, 2015; Suyker & Verma, 2012) (Table 4).

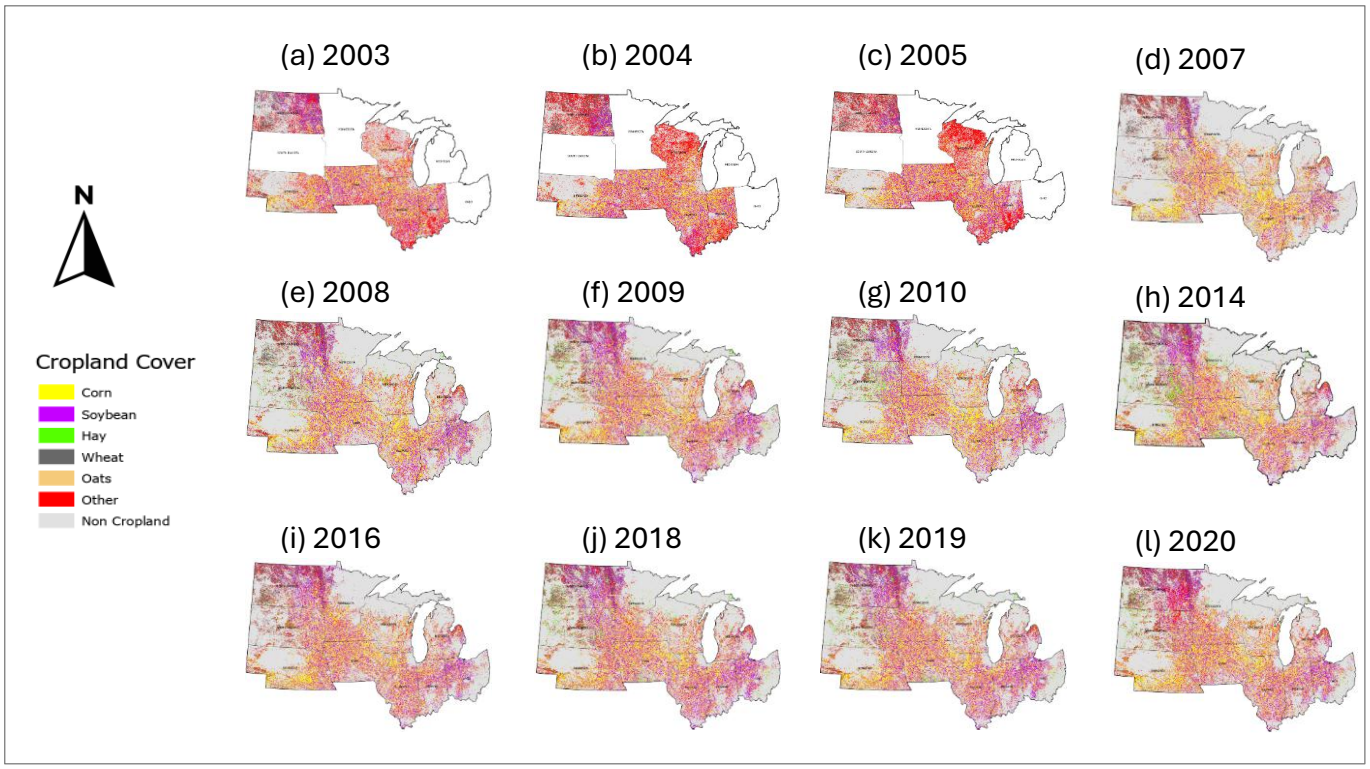


**Figure 13.** Cropland cover of no significant drought years. Figure describing corn, soybean, hay, wheat, oats and other cropland over Corn Belt Region. (a) 2003, (b) 2004, (c) 2005, (d) 2007, (e) 2008, (f) 2009, (g) 2010, (h) 2014, (i) 2016, (j) 2018, (k) 2019, (l) 2020 crop cover years. Crop cover is not a measure of drought impacts but of crop rotation, plantations, and depletion.

In crop quantities, the overall distribution of crop cover showed more cropland cover of overall distribution, displaying more than seven-eighths of the overall distribution as evidenced by missing data (2003–2005), but then started to decrease from 2007–2015 (Green *et al.*, 2018). High quantities of corn and soybeans were dominant in 2016 and 2018, showing exactly one-quarter of the distribution, but decreased slightly to less than one-quarter in 2019 and 2020. (Figure 14).

**Table 4.** Crop production thresholds of no significant drought. Table 4 describes the impacts of corn and soybeans for the years impacted by non-significant drought in the Corn Belt Region. The table demonstrates crop productivity as a result of non-drought to considerable wetness in the region.

| Year | Nebraska | Iowa | South Dakota | North Dakota | Minnesota | Illinois | Wisconsin | Indiana | Michigan | Ohio |
|---|---|---|---|---|---|---|---|---|---|---|
| Corn | | | | | | | | | | |
| 2003 | 51 | 43 | 56 | 41 | 53 | 67 | 33 | 65 | 60 | 74 |
| 2004 | 80 | 76 | 74 | 36 | 63 | 84 | 57 | 84 | 55 | 73 |
| 2005 | 67 | 77 | 62 | 70 | 75 | 22 | 65 | 54 | 66 | 47 |
| 2007 | 82 | 73 | 73 | 74 | 46 | 77 | 46 | 52 | 31 | 51 |
| 2008 | 77 | 65 | 78 | 70 | 67 | 72 | 61 | 59 | 54 | 38 |
| 2009 | 80 | 69 | 71 | 62 | 49 | 62 | 62 | 56 | 71 | 76 |
| 2010 | 81 | 70 | 74 | 84 | 87 | 53 | 84 | 56 | 74 | 63 |
| 2014 | 76 | 76 | 74 | 73 | 66 | 84 | 72 | 77 | 72 | 78 |
| 2016 | 73 | 83 | 57 | 83 | 87 | 83 | 86 | 70 | 67 | 47 |
| 2018 | 79 | 69 | 72 | 66 | 76 | 80 | 68 | 70 | 56 | 82 |
| 2019 | 73 | 67 | 65 | 52 | 57 | 55 | 67 | 36 | 42 | 37 |
| 2020 | 59 | 47 | 78 | 59 | 80 | 66 | 81 | 62 | 65 | 51 |
| Soybean | | | | | | | | | | |
| 2003 | 27 | 16 | 47 | - | 21 | 46 | 16 | 45 | 37 | 57 |
| 2004 | 63 | 73 | 65 | - | 47 | 76 | 58 | 78 | 54 | 68 |
| 2005 | 61 | 77 | 63 | - | 73 | 34 | 56 | 57 | 56 | 59 |
| 2007 | 80 | 76 | 73 | - | 56 | 77 | 61 | 43 | 38 | 54 |
| 2008 | 70 | 62 | 66 | - | 56 | 72 | 46 | 49 | 37 | 28 |
| 2009 | 80 | 69 | 71 | - | 62 | 62 | 49 | 62 | 56 | 71 |
| 2010 | 78 | 73 | 67 | - | 84 | 53 | 83 | 54 | 70 | 59 |
| 2014 | 75 | 73 | 77 | - | 67 | 80 | 71 | 75 | 60 | 75 |
| 2016 | 77 | 81 | 65 | - | 83 | 82 | 85 | 77 | 72 | 63 |
| 2018 | 79 | 66 | 61 | - | 72 | 81 | 72 | 71 | 73 | 78 |
| 2019 | 71 | 66 | 57 | - | 54 | 49 | 64 | 33 | 44 | 35 |
| 2020 | 66 | 49 | 68 | - | 78 | 67 | 82 | 63 | 67 | 57 |

# 4. Conclusions

This research was designed to investigate the effects of precipitation regimes on drought severity and their influence on crop yield and production (Sun *et al.*, 2023). This research demonstrated the need to assess the parameters of wetness and dryness regimes given by the index of SPI. In this research, the focus of this paper was on the climate and weather effects dedicated to drought assessment and its impact on crop production and yield from 2000 to 2023, as categorized through the four classification groups. While the three classifications were under drought, one class was under non-significant drought.

This research indicated a clear picture of widespread coverage and intensity, followed by numerous pockets of drought conditions throughout the region. Drought coverage and severity were widespread and numerous throughout both regions, mainly for extreme, severe, and moderate drought categories (Hosseini *et al.*, 2021; Li *et al.*, 2020; Shrestha *et al.*, 2020). In extreme cases, 2002, 2006, 2012, and 2013


**Figure 14.** Total landcover distribution of no significant drought years. Crop quantities of corn (orange), soybean (green), and total overall crop distribution of the Corn Belt Region. Not a reflection of drought impacts.

experienced widespread impacts, especially in 2012, where most of the region was under widespread extreme dryness. For non-drought, a persistent wet pattern started to plague the region, especially during the last two-thirds of the period, especially in 2010, 2014, and 2016. These years indicated perhaps the most significant patterns of wetness, especially along the Western Corn Belt of the western Great Plains and the northern Great Lakes Region (Auch *et al.*, 2013; Green *et al.*, 2018; Ort & Long, 2014; Panagopoulos *et al.*, 2015; Suyker & Verma, 2012). This analysis concluded that the research results support the evidence of drought severity and its influence on crop production. Specifically, climate change can alter weather patterns, leading to drought stress among plants such as corn and soybeans (Fadhli *et al.*, 2020; Green *et al.*, 2018; Sakellariou *et al.*, 2024). In this research, the four classifications correlated well with the results in terms of crop production. As crop production varied between the crop types, results revealed similar patterns in terms of the different regimes of these classes. Specifically, the corn and soybean yields were plentiful throughout the

period (S. Li *et al.*, 2021; Peña-Gallardo *et al.*, 2019; Prince *et al.*, 2001). While missing data affected the overall results, heavy concentrations of crop diversity were widespread, especially during the early decadal period of some of the drought classes, especially in the corn and soybean distribution cover. Overall, corn and soybeans mixed with oats (later in the period) were distributed along the southern corn belt states. The analysis showed that these widespread and intense drought episodes impacted crop production. While drought conditions were numerous, crop yields were severely affected in the region throughout these drought periods, especially in 2002, 2012, and 2021 (Aghelpour *et al.*, 2021; Peña-Gallardo *et al.*, 2019; Prince *et al.*, 2001; Yoon *et al.*, 2020). The most significant impacts were between 2002 and 2012 and 2021, indicating the lowest yields of both crops compared to any other year. Non-drought years indicated numerous above to well above average levels of wealthy crop production for both crops. Crop production indicated wealthier conditions throughout the period, with 2010 and 2016 indicating the most significant levels than any other year, especially along the northern Great Lakes states from North Dakota and Minnesota stretching southeastward towards Illinois (Green *et al.*, 2018; Ort & Long, 2014; Panagopoulos *et al.*, 2015; Suyker & Verma, 2012).

Overall, this research supported the need to understand the four drought types. It also demonstrated the hypothesis that meteorological drought is the leading drought type influencing the economic, environmental, and social sectors. Therefore, extreme climate events such as drought and extreme precipitation have been on the rise in other countries and other sections of the western hemisphere (Gattoni *et al.*, 2025; McGranahan & Wonkka, 2024; Weaver & Bruner, 1948). This research supports the evidence that there has been an increase in drought conditions and that the severity and intensity of drought has increased, especially in the concentrated corn and soybean belts, with an uptick in wet conditions along the Great Plains to the northern Great Lakes (L. Li *et al.*, 2020; Shrestha *et al.*, 2020; Wahl *et al.*, 2022). This research has also demonstrated the need to understand further drought and its impacts on crop yield, allowing communities to provide adaptation measures for resiliency and mitigation responses for future occurrences of drought in the future (Leeper *et al.*, 2022; L. Li *et al.*, 2020; Shiru *et al.*, 2019; Shrestha *et al.*, 2020).

**Data Availability Statement**: Data, climate, cropland cover, and yield are available online for open-access use at https://climatedataguide.ucar.edu/climate-data/chirps-climate-hazards-infrared-precipitation-station-data-version-2, crop cover data - https://nassgeodata.gmu.edu/, and yield data - https://www.nass.usda.gov/Data_and_Statistics/index.php, and crop yield data https://www.nass.usda.gov/Research_and_Science/Cropland/SARS1a.php for data-ready access.

**Acknowledgment**: Funded by the University of North Dakota and North DakotaView. This material is based upon work supported partly by the U.S. Geological Survey under Grant/Cooperative Agreement No. G18AP00077 (for GY18-GY22) or G23AP00683 (GY23-GY27).

**Conflicts of Interest**: The authors declare no conflicts of interest. The funders had no role in the design of the study; in the collection, analyses, or interpretation of data; in the writing of the manuscript; or in the decision to publish the results.

# References

Acharki, S., Singh, S. K., do Couto, E. V., Arjdal, Y., & Elbeltagi, A. (2023). Spatio-temporal distribution and prediction of agricultural and meteorological drought in a Mediterranean coastal watershed via GIS and machine learning. *Physics and Chemistry of the Earth, Parts A/B/C*, *131*, 103425. https://doi.org/10.1016/j.pce.2023.103425

Aghelpour, P., Mohammadi, B., Mehdizadeh, S., Bahrami-Pichaghchi, H., & Duan, Z. (2021). A novel hybrid dragonfly optimization algorithm for agricultural drought prediction. *Stochastic Environmental Research and Risk Assessment*, *35*(12), 2459–2477. https://doi.org/10.1007/s00477-021-02011-2

Angelidis, P., Maris, F., Kotsovinos, N., & Hrissanthou, V. (2012). Computation of drought index SPI with alternative distribution functions. *Water Resources Management*, *26*(9), 2453–2473. https://doi.org/10.1007/s11269-012-0026-0

Auch, R. F., Laingen, C., Drummond, M. A., Sayler, K. L., Reker, R. R., Bouchard, M. A., & Danielson, J. J. (2013). Land-use and land-cover change in three Corn Belt ecoregions: Similarities and differences. *Focus on Geography*, *56*(4), 135–143. https://doi.org/10.1111/foge.12022

Ayugi, B., Eresanya, E. O., Onyango, A. O., Ogou, F. K., Okoro, E. C., Okoye, C. O., Anoruo, C. M., Dike, V. N., Ashiru, O. R., Daramola, M. T., Mumo, R., & Ongoma, V. (2022). Review of meteorological drought in Africa: Historical trends, impacts,

mitigation measures, and prospects. *Pure and Applied Geophysics*, *179*(4), 1365–1386. https://doi.org/10.1007/s00024-022-02988-z

Boryan, C., Yang, Z., Mueller, R., & Craig, M. (2011). Monitoring US agriculture: The US Department of Agriculture, National Agricultural Statistics Service, Cropland Data Layer Program. *Geocarto International*, *26*(5), 341–358. https://doi.org/10.1080/10106049.2011.562309

Bouaziz, M., Medhioub, E., & Csaplovisc, E. (2021). A machine learning model for drought tracking and forecasting using remote precipitation data and a standardized precipitation index from arid regions. *Journal of Arid Environments*, *189*, 104478. https://doi.org/10.1016/j.jaridenv.2021.104478

Brandes, E., McNunn, G. S., Schulte, L. A., Bonner, I. J., Muth, D. J., Babcock, B. A., Sharma, B., & Heaton, E. A. (2016). Subfield profitability analysis reveals an economic case for cropland diversification. *Environmental Research Letters*, *11*(1), 014009. https://doi.org/10.1088/1748-9326/11/1/014009

Chen, M., Kumar, A., L'Heureux, M., Peng, P., Zhang, T., Hoerling, M. P., & Diaz, H. F. (2024). Why do DJF 2023/24 upper-level 200-hPa geopotential height forecasts look different from the expected El Niño response? *Geophysical Research Letters*, *51*(14), e2024GL108946. https://doi.org/10.1029/2024GL108946

de Oliveira-Júnior, J. F., da Silva Junior, C. A., Teodoro, P. E., Rossi, F. S., Blanco, C. J. C., Lima, M., de Gois, G., Correia Filho, W. L. F., de Barros Santiago, D., & dos Santos Vanderley, M. H. G. (2021). Confronting CHIRPS dataset and in situ stations in the detection of wet and drought conditions in the Brazilian Midwest. *International Journal of Climatology*, *41*(9), 4478–4493. https://doi.org/10.1002/joc.7080

de Oliveira-Júnior, J. F., Mendes, D., Porto, H. D., Cardoso, K. R. A., Neto, J. A. F., da Silva, E. B. C., de Aquino Pereira, M., Mendes, M. C. D., Baracho, B. B. D., & Jamjareegulgarn, P. (2025). Analysis of drought and extreme precipitation events in Thailand: Trends, climate modeling, and implications for climate change adaptation. *Scientific Reports*, *15*(1), 4501. https://doi.org/10.1038/s41598-025-86826-x

Du, H., Tan, M. L., Zhang, F., Chun, K. P., Li, L., & Kabir, M. H. (2024). Evaluating the effectiveness of CHIRPS data for hydroclimatic studies. *Theoretical and Applied Climatology*, *155*(3), 1519–1539. https://doi.org/10.1007/s00704-023-04721-9

Duffy, P. B., Brando, P., Asner, G. P., & Field, C. B. (2015). Projections of future meteorological drought and wet periods in the Amazon. *Proceedings of the National Academy of Sciences*, *112*(43), 13172–13177. https://doi.org/10.1073/pnas.1421010112

Fadhli, N., Farid, Muh., Rafiuddin, Effendi, R., Azrai, M., & Anshori, M. F. (2020). Multivariate analysis to determine secondary characters in selecting adaptive hybrid corn lines under drought stress. *Biodiversitas Journal of Biological Diversity*, *21*(8). https://doi.org/10.13057/biodiv/d210826

Fenneman, N. M. (1917). Physiographic subdivision of the United States. *Proceedings of the National Academy of Sciences*, *3*(1), 17–22. https://doi.org/10.1073/pnas.3.1.17

Funk, C., Peterson, P., Landsfeld, M., Pedreros, D., Verdin, J., Shukla, S., Husak, G., Rowland, J., Harrison, L., Hoell, A., & Michaelsen, J. (2015). The climate hazards infrared precipitation with stations—A new environmental record for monitoring extremes. *Scientific Data*, *2*(1), 150066. https://doi.org/10.1038/sdata.2015.66

Gattoni, K., Gendron, E. M. S., McQueen, J. P., Powers, K., Powers, T. O., Harner, M. J., Corman, J. R., & Porazinska, D. L. (2025). The nature of microbial diversity and assembly in the Nebraska Sandhills depends on organismal identity and habitat type. *Community Ecology*, *26*(1), 1–14. https://doi.org/10.1007/s42974-024-00206-5

Green, T. R., Kipka, H., David, O., & McMaster, G. S. (2018). Where is the USA Corn Belt, and how is it changing? *Science of The Total Environment*, *618*, 1613–1618. https://doi.org/10.1016/j.scitotenv.2017.09.325

Guttman, N. B. (1998). Comparing the Palmer drought index and the standardized precipitation index 1. *JAWRA Journal of the American Water Resources Association*, *34*(1), 113–121. https://doi.org/10.1111/j.1752-1688.1998.tb05964.x

Guttman, N. B. (1999). Accepting the standardized precipitation index: A calculation algorithm 1. *JAWRA Journal of the American Water Resources Association*, *35*(2), 311–322. https://doi.org/10.1111/j.1752-1688.1999.tb03592.x

Han, W., Yang, Z., Di, L., & Mueller, R. (2012). CropScape: A Web service based application for exploring and disseminating US conterminous geospatial cropland data products for decision support. *Computers and Electronics in Agriculture*, *84*, 111–123. https://doi.org/10.1016/j.compag.2012.03.005

Hosseini, A., Ghavidel, Y., Mohammad Khorshiddoust, A., & Farajzadeh, M. (2021). Spatio-temporal analysis of dry and wet periods in Iran by using Global Precipitation Climatology Center-Drought Index (GPCC-DI). *Theoretical and Applied Climatology*, *143*(3–4), 1035–1045. https://doi.org/10.1007/s00704-020-03463-2

Leeper, R. D., Bilotta, R., Petersen, B., Stiles, C. J., Heim, R., Fuchs, B., Prat, O. P., Palecki, M., & Ansari, S. (2022). Characterizing U.S. drought over the past 20 years using the U.S. drought monitor. *International Journal of Climatology*, *42*(12), 6616–6630. https://doi.org/10.1002/joc.7653

Li, L., She, D., Zheng, H., Lin, P., & Yang, Z.-L. (2020). Elucidating diverse drought characteristics from two meteorological drought indices (SPI and SPEI) in China. *Journal of Hydrometeorology*, *21*(7), 1513–1530. https://doi.org/10.1175/JHM-D-19-0290.1

Li, S., Thompson, M., Moussavi, S., & Dvorak, B. (2021). Life cycle and economic assessment of corn production practices in the western US Corn Belt. *Sustainable Production and Consumption*, *27*, 1762–1774. https://doi.org/10.1016/j.spc.2021.04.021

Liu, C., Yang, C., Yang, Q., & Wang, J. (2021). Spatiotemporal drought analysis by the standardized precipitation index (SPI) and standardized precipitation evapotranspiration index (SPEI) in Sichuan Province, China. *Scientific Reports*, *11*(1), 1280. https://doi.org/10.1038/s41598-020-80527-3

Liu, L., Hong, Y., Looper, J., Riley, R., Yong, B., Zhang, Z., Hocker, J., & Shafer, M. (2013). Climatological drought analyses and projection using SPI and PDSI: Case study of the Arkansas Red River Basin. *Journal of Hydrologic Engineering*, *18*(7), 809–816. https://doi.org/10.1061/(ASCE)HE.1943-5584.0000619

Lloyd-Hughes, B., & Saunders, M. A. (2002). A drought climatology for Europe. *International Journal of Climatology*, *22*(13), 1571–1592. https://doi.org/10.1002/joc.846

López-Bermeo, C., Montoya, R. D., Caro-Lopera, F. J., & Díaz-García, J. A. (2022). Validation of the accuracy of the CHIRPS precipitation dataset at representing climate variability in a tropical mountainous region of South America. *Physics and Chemistry of the Earth, Parts A/B/C*, *127*, 103184. https://doi.org/10.1016/j.pce.2022.103184

McGranahan, D. A., & Wonkka, C. L. (2024). Pyrogeography of the Western Great Plains: A 40-year history of fire in semi-arid rangelands. *Fire*, *7*(1), Article 1. https://doi.org/10.3390/fire7010032

Meresa, H., Zhang, Y., Tian, J., & Abrar Faiz, M. (2023). Understanding the role of catchment and climate characteristics in the propagation of meteorological to hydrological drought. *Journal of Hydrology*, *617*, 128967. https://doi.org/10.1016/j.jhydrol.2022.128967

Mishra, A. K., & Singh, V. P. (2010). A review of drought concepts. *Journal of Hydrology*, *391*(1), 202–216. https://doi.org/10.1016/j.jhydrol.2010.07.012

Ort, D. R., & Long, S. P. (2014). Limits on yields in the Corn Belt. *Science*, *344*(6183), 484–485. https://doi.org/10.1126/science.1253884

Panagopoulos, Y., Gassman, P. W., Jha, M. K., Kling, C. L., Campbell, T., Srinivasan, R., White, M., & Arnold, J. G. (2015). A refined regional modeling approach for the Corn Belt – Experiences and recommendations for large-scale integrated modeling. *Journal of Hydrology*, *524*, 348–366. https://doi.org/10.1016/j.jhydrol.2015.02.039

Peña-Gallardo, M., Vicente-Serrano, S. M., Quiring, S., Svoboda, M., Hannaford, J., Tomas-Burguera, M., Martín-Hernández, N., Domínguez-Castro, F., & El Kenawy, A. (2019). Response of crop yield to different time-scales of drought in the United States: Spatio-temporal patterns and climatic and environmental drivers. *Agricultural and Forest Meteorology*, *264*, 40–55. https://doi.org/10.1016/j.agrformet.2018.09.019

Prince, S. D., Haskett, J., Steininger, M., Strand, H., & Wright, R. (2001). Net primary production of U.S. Midwest croplands from agricultural harvest yield data. *Ecological Applications*, *11*(4), 1194–1205. https://doi.org/10.1890/1051-0761(2001)011[1194:NPPOUS]2.0.CO;2

Rosenberg, N. J. (1987). Climate of the Great Plains Region of the United States. *Great Plains Quarterly*, *7*(1), 22–32.

Sakellariou, S., Spiliotopoulos, M., Alpanakis, N., Faraslis, I., Sidiropoulos, P., Tziatzios, G. A., Karoutsos, G., Dalezios, N. R., & Dercas, N. (2024). Spatiotemporal drought assessment based on gridded Standardized Precipitation Index (SPI) in vulnerable agroecosystems. *Sustainability*, *16*(3), 1240. https://doi.org/10.3390/su16031240

Schneider, D. P., Deser, C., Fasullo, J., & Trenberth, K. E. (2013). Climate Data Guide spurs discovery and understanding. *Eos, Transactions American Geophysical Union*, *94*(13), 121–122. https://doi.org/10.1002/2013EO130001

Sharafati, A., Nabaei, S., & Shahid, S. (2020). Spatial assessment of meteorological drought features over different climate regions in Iran. *International Journal of Climatology*, *40*(3), 1864–1884. https://doi.org/10.1002/joc.6307

Shiru, M. S., Shahid, S., Chung, E.-S., & Alias, N. (2019). Changing characteristics of meteorological droughts in Nigeria during 1901–2010. *Atmospheric Research*, *223*, 60–73. https://doi.org/10.1016/j.atmosres.2019.03.010

Shrestha, A., Rahaman, M. M., Kalra, A., Jogineedi, R., & Maheshwari, P. (2020). Climatological drought forecasting using bias corrected CMIP6 climate data: A case study for India. *Forecasting*, *2*(2), 59–84. https://doi.org/10.3390/forecast2020004

Sönmez, F. Kemal., Kömüscü, A. Ü., Erkan, A., & Turgu, E. (2005). An analysis of spatial and temporal dimension of drought vulnerability in Turkey using the Standardized Precipitation Index. *Natural Hazards*, *35*(2), 243–264. https://doi.org/10.1007/s11069-004-5704-7

Stagge, J. H., Tallaksen, L. M., Gudmundsson, L., Van Loon, A. F., & Stahl, K. (2015). Candidate distributions for climatological drought indices (SPI and SPEI). *International Journal of Climatology*, *35*(13), 4027–4040. https://doi.org/10.1002/joc.4267

Sun, P., Liu, R., Yao, R., Shen, H., & Bian, Y. (2023). Responses of agricultural drought to meteorological drought under different climatic zones and vegetation types. *Journal of Hydrology*, *619*, 129305. https://doi.org/10.1016/j.jhydrol.2023.129305

Suyker, A. E., & Verma, S. B. (2012). Gross primary production and ecosystem respiration of irrigated and rainfed maize–soybean cropping systems over 8 years. *Agricultural and Forest Meteorology*, *165*, 12–24. https://doi.org/10.1016/j.agrformet.2012.05.021

Tsiros, I. X., Nastos, P., Proutsos, N. D., & Tsaousidis, A. (2020). Variability of the aridity index and related drought parameters in Greece using climatological data over the last century (1900–1997). *Atmospheric Research*, *240*, 104914. https://doi.org/10.1016/j.atmosres.2020.104914

Wahl, E. R., Zorita, E., Diaz, H. F., & Hoell, A. (2022). Southwestern United States drought of the 21st century presages drier conditions into the future. *Communications Earth & Environment*, *3*(1), 202. https://doi.org/10.1038/s43247-022-00532-4

Wang, F., Lai, H., Li, Y., Feng, K., Zhang, Z., Tian, Q., Zhu, X., & Yang, H. (2022). Dynamic variation of meteorological drought and its relationships with agricultural drought across China. *Agricultural Water Management*, *261*, 107301. https://doi.org/10.1016/j.agwat.2021.107301

Weaver, J. E., & Bruner, W. E. (1948). Prairies and pastures of the dissected loess plains of central Nebraska. *Ecological Monographs*, *18*(4), 507–549. https://doi.org/10.2307/1948587

Wilhite, D. A., & Glantz, M. H. (1985). Understanding the drought phenomenon: The role of definitions. *Water International*, *10*(3), 111–120. https://doi.org/10.1080/02508068508686328

Wilson, A. B., Avila-Diaz, A., Oliveira, L. F., Zuluaga, C. F., & Mark, B. (2022). Climate extremes and their impacts on agriculture across the Eastern Corn Belt Region of the U.S. *Weather and Climate Extremes*, *37*, 100467. https://doi.org/10.1016/j.wace.2022.100467

Yoon, D.-H., Nam, W.-H., Lee, H.-J., Hong, E.-M., Feng, S., Wardlow, B. D., Tadesse, T., Svoboda, M. D., Hayes, M. J., & Kim, D.-E. (2020). Agricultural drought assessment in East Asia using satellite-based indices. *Remote Sensing*, *12*(3), Article 3. https://doi.org/10.3390/rs12030444